Regular Article

Development of Functional Chimeric Nanoparticles by Membrane Fusion of Small Extracellular Vesicles and Drug-Encapsulated Liposomes

Tatsuya Fukuta,*[a] Akina Nishikawa,[b] Ami Hiramachi,[c] Sachika Yamashita,[c] and Kentaro Kogure[d]

[a] *Department of Physical Pharmaceutics, School of Pharmaceutical Sciences, Wakayama Medical University, 25–1 Shichiban-cho, Wakayama 640–8156, Japan:* [b] *Faculty of Pharmaceutical Sciences, Tokushima University, 1–78–1 Shomachi, Tokushima 770–8505, Japan:* [c] *Graduate School of Pharmaceutical Sciences, Tokushima University, 1–78–1 Shomachi, Tokushima 770–8505, Japan: and* [d] *Graduate School of Biomedical Sciences, Tokushima University, 1–78–1 Shomachi, Tokushima 770–8505, Japan.*

Received February 27, 2023; accepted June 6, 2023

Since small extracellular vesicle (sEVs) are involved in cell-to-cell communication *via* transfer of certain bioactive molecules and have the capability to overcome biological barriers against drug transport, their use as a drug delivery system (DDS) has been demonstrated in treatment of a diverse range of diseases. However, some issues in drug encapsulation have been pointed out, including low encapsulation efficiency and poor reproducibility. It was previously reported that liposomes containing phosphatidylserine (PS) can fuse together in the presence of calcium ion, which allows for drug encapsulation into the resultant liposomes (*i.e.*, calcium fusion method). On the other hand, PS is reportedly present in lipid membrane of sEVs as a distinct lipid composition. We therefore hypothesized that PS-mediated membrane fusion of sEVs with PS-liposomes encapsulating therapeutic agents *via* the calcium fusion method can be applied to convenient drug encapsulation into sEVs. Membrane fusion of PS-liposomes and sEVs derived from murine melanoma B16F1 cells (B16-sEVs) was firstly confirmed. The obtained nanoparticles, termed chimeric nanoparticles (CM-NP), showed comparable cellular uptake to B16-sEVs into B16F1 cells. Moreover, CM-NP encapsulating an anticancer drug doxorubicin (DOX) (CM-NP-DOX) could be prepared by membrane fusion of PS-liposomes encapsulating DOX (PS-Lipo-DOX) and B16-sEVs. CM-NP-DOX exhibited a superior anticancer effect on B16F1 cells *in vitro* compared with PS-Lipo-DOX. These findings suggest that the calcium fusion method could be applied for membrane fusion of sEVs and PS-liposomes, and that this approach would likely be useful for efficient drug encapsulation into sEVs, as well as increasing liposome functionality.

Key words small extracellular vesicle, liposome, drug delivery system, phosphatidylserine, calcium fusion

INTRODUCTION

Small extracellular vesicles (sEVs) are cell-derived vesicles with lipid bilayer membrane having 40–150 nm in diameter.[1] They are related to cell-to-cell communication *via* transfer of encapsulated bioactive components, such as nucleic acids and proteins, to recipient cells.[2] Numerous membrane proteins are expressed on exosomal surfaces and exhibit not only targeting capabilities to specific tissues/cells stemmed from properties of donor cells, but also ability to pass through biological barriers (*e.g.*, the blood-brain barrier).[3,4] Because of the above characteristics, use of sEVs in therapeutic application and as a drug delivery system (DDS) has been expected.

To apply sEVs as a DDS, encapsulating low molecular weight or macromolecular drugs has been reported in many studies by several methods, such as incubation of sEVs with drug solution, membrane permeabilization with detergents, and use of physical treatments (*e.g.*, electroporation, sonication).[5] The usefulness of these drug-encapsulated sEVs has been demonstrated in the treatment of various diseases.[6] Meanwhile, some issues in drug encapsulation have been pointed out, including low encapsulation efficiency and poor reproducibility,[5] and improvement of these issues is required. Liposomes, which are composed of lipid membranes similar to sEVs, have been used for disease therapy with the development of many drug encapsulation and functional ligand modification methods.[7] Among them, the calcium fusion method was previously employed for encapsulation of soluble compounds, including dextran and DNA, into liposomes,[8] in which liposomes containing a phospholipid phosphatidylserine (PS) fuse together in the presence of calcium ions, followed by obtaining unilamellar liposomes by treating with a calcium chelating agent, ethylenediaminetetraacetic acid (EDTA).[9] On the other hand, PS has been reported to exist in the lipid membrane of sEVs as a distinct lipid composition,[10] and an affinity isolation method of sEVs using PS displayed on their surfaces was also previously developed.[11] By focusing on the presence of PS on membranes of sEVs, we hypothesized that PS-mediated membrane fusion of sEVs with PS-liposomes encapsulating drugs *via* the calcium fusion can be applied to convenient drug encapsulation into sEVs. Also, their membrane fusion may impart unique properties of sEVs (*e.g.*, high cellular uptake efficiency) to liposomes, allowing for development of nanoparticles possessing functions derived from both sEVs and liposomes.

In this study, by using liposomes composed of different PS compositions and sEVs derived from murine melanoma B16F1 cells (B16-sEVs), we first investigated whether membrane fusion of those liposomes and sEVs can be achieved by the calcium fusion method. Cellular uptake of the prepared fused nanoparticles, here termed chimeric nanoparticles (CM-NP), into B16F1 cells was then evaluated and compared with plain

* To whom correspondence should be addressed. e-mail: fukuta@wakayama-med.ac.jp

PS-liposomes and B16-sEVs. In addition, CM-NP encapsulating an anticancer drug doxorubicin (DOX) was prepared by membrane fusion of PS-liposomes encapsulating DOX and B16-sEVs, and its anticancer effect was evaluated *in vitro*.

MATERIALS AND METHODS

Cell Culture Mouse melanoma B16F1 cells were purchased from DS Pharma Biomedical (Osaka, Japan). B16F1 cells were cultivated in Dulbecco's modified Eagle Medium (DMEM; Nacalai Tesque, Kyoto, Japan) containing 100 U/mL penicillin and 100 μg/mL streptomycin (Gibco, MA, U.S.A.) and 10% fetal bovine serum (FBS), and cultured at 37 °C in a 5% CO_2 incubator.

Collection of sEVs B16F1 cells were seeded (2×10^6 cells/dish) onto 150-mm dishes and cultured for 24 h. The cells were then rinsed using phosphate-buffered saline (PBS), and media were changed to FBS-free advanced DMEM (Gibco) containing 100 U/mL penicillin and 100 μg/mL streptomycin and 2 mM L-glutamine (Gibco). The culture supernatant was collected 48 h after incubation, and B16F1-derived sEVs (B16-sEVs) were collected as previously reported.[12] In brief, the collected medium was sequentially centrifuged at $300 \times \boldsymbol{g}$ for 10 min, $2000 \times \boldsymbol{g}$ for 20 min, and $10000 \times \boldsymbol{g}$ for 30 min at 4 °C, and filtered with 0.22-μm syringe filters. The medium was then ultracentrifuged at $100000 \times \boldsymbol{g}$ for 70 min at 4 °C (Optima L-90K; Beckman Coulter, Tokyo, Japan) to pellet B16-sEVs, followed by resuspension in PBS and ultracentrifugation. The obtained B16-sEVs were resuspended in PBS and then used in experiments.

Preparation of Liposomes Egg phosphatidylcholine (EPC) and dioleoylphosphatidylserine (DOPS) were both purchased from NOF Corporation (Tokyo, Japan). Lissamine rhodamine B (Rhodamine)-labeled dioleoylphosphatidylethanolamine (DOPE) and *N*-(7-nitro-2-1,3-benzoxadiazol-4-yl) (NBD)-labeled DOPE were purchased from Avanti Polar Lipids (Alabaster, AL, U.S.A.). Liposomes composed of each molar ratio of EPC/DOPS (10/0, 9/1, 7.5/2.5, and 5/5 M ratio) were prepared by the thin-film method. Compositions of the liposomes were termed PS0-, PS10-, PS25-, and PS50-Lipo, respectively. The lipid solution prepared in chloroform/methanol was added to test tubes and dried by use of nitrogen gas. For fluorescent labeling, Rhodamine- and NBD-labeled DOPE were mixed in the lipid solution at 1 mol% concentration of total lipid, respectively. The lipid film was hydrated with PBS, and the resultant liposomes were passed through a mini-extruder with polycarbonate membrane filters having 100 nm pores (Avanti Polar Lipids). The particle size, polydispersity index (PDI), and ζ-potential of the liposomes were determined using a Zetasizer Nano ZS (Malvern Instruments, Worcestershire, U.K.).

Membrane Fusion by the Calcium Fusion Method Calcium fusion of PS-liposomes and B16-sEVs was performed by the calcium fusion method with modifications.[8] Briefly, 250 μL of each composition of 100 μM liposomes and 250 μL B16-sEVs suspension (30 μg as protein amount) were mixed, followed by addition of 500 μL 20 mM $CaCl_2$ in ultrapure water (Final $CaCl_2$ conc. 10 mM). After incubation for 1 h at 37 °C, those samples were mixed with 500 μL 30 mM EDTA in PBS, vortexed for 10 s, and incubated for 30 min at 37 °C. Depending on the experiments, liposomes were labeled with NBD-DOPE, Rhodamine-DOPE, or both, and B16-sEVs with a fluorescent probe PKH67 (Sigma-Aldrich, MO, U.S.A.) in accordance with the manufacturer's protocol.

Fluorescence Resonance Energy Transfer (FRET) Assay Membrane fusion of B16-sEVs and each liposome labeled with NBD-DOPE (excitation: 460 nm, emission: 530 nm) and Rhodamine-DOPE (excitation: 543 nm, emission: 590 nm) was assessed by a FRET assay.[13] NBD excitation at 460 nm induces Rhodamine emission at 590 nm under the FRET condition in liposomal membranes, while lipid dilution upon membrane fusion with B16-sEVs increases the distances between the FRET fluorophores and decreases Rhodamine emission. The FRET between each liposome and B16-sEVs was monitored by scanning fluorescence intensity from 510 to 650 nm every 10 nm following NBD excitation at 460 nm with a Tecan Infinite M200 microplate reader (Salzburg, Switzerland). The decrease percentage of the FRET fluorescence was calculated with the following equation: 100 − fluorescence intensity at 590 nm after calcium fusion ÷ fluorescence intensity at 590 nm after the same procedure without $CaCl_2$ and EDTA × 100 (%).

Density Gradient Ultracentrifugation Rhodamine-labeled PS0- or PS25-Lipo were mixed with PKH67-labeled B16-sEVs and subjected to calcium fusion treatment, as described above. The samples (1 mL) were layered on iodixanol (Optiprep™, Sigma-Aldrich) density gradient prepared with 2 mL 5% iodixanol, 3.5 mL 10% iodixanol, 4 mL 20% iodixanol, and 1.5 mL 40% iodixanol in 0.25M sucrose containing 10 mM Tris–HCl (pH 7.5), followed by ultracentrifugation with SW41Ti swing rotor (Beckman Coulter) at $100000 \times \boldsymbol{g}$ for 18 h at 4 °C. Each sample was then divided into 11 fractions and fluorescence intensities of Rhodamine (excitation: 543 nm, emission: 588 nm) and PKH67 (excitation: 488 nm, emission, 520 nm) were measured with a microplate reader. Based on the results of fluorescence measurement of Rhodamine and PKH67 in each fraction, we calculated membrane fusion efficiency of liposomes and sEVs according to the following formula:

$$\begin{aligned}&\text{Membrane fusion efficiency}(\%)\\&= \text{Rhodamine fluorescence values in the liposome fractions coexisting with the sEVs fractions after fusion treatment (Fusion (+))} \div \text{Total Rhodamine fluorescence values observed in all fractions} \times 100.\end{aligned}$$

Cellular Uptake of CM-NPs B16F1 cells were seeded (1.5×10^5 cells/dish) onto 35-mm glass bottom dishes and cultured at 37 °C for 24 h. Each sample labeled with PKH67 was added to the cells (Final concentration: 8.3 μM as liposomes and 10 μg/mL as B16-sEVs in DMEM containing 10% FBS) and incubated for 24 h. The cells were washed with PBS twice and fixed with 4% paraformaldehyde for 10 min at 37 °C, followed by nuclear staining using 4′6-diamidino-2-phenylindole (DAPI; Thermo Fisher Scientific, Waltham, MA, U.S.A.) diluted in PBS at a concentration of 1 μg/mL at 37 °C for 15 min. Thereafter, fluorescence of PKH67 and DAPI in the cells was observed by confocal laser scanning microscopy (LSM700, Carl Zeiss, Jena, Germany).

In case of quantitative analyses, B16F1 cells were seeded (3.0×10^4 cells/well) onto 24-well plates and cultivated at 37 °C overnight. After treatment with the PKH67-labeled samples as mentioned above for 6 and 24 h, the cells were rinsed in PBS and lysed using 1% *n*-octyl-β-D-glucoside (Dojindo,

Kumamoto, Japan). The fluorescence intensity of PKH67 was measured with a microplate reader. Cellular uptake (%) was calculated according to the following equation:

PKH67 fluorescence intensity of cellular lysates
÷ PKH67 fluorescence intensity of the added samples × 100 (%).

Preparation of CM-NP Encapsulating Doxorubicin Encapsulation of DOX into liposomes was performed as previously reported.[14] Briefly, a lipid film composed of EPC/DOPS (3/1 M ratio) was hydrated using 250 mM ammonium sulfate, and the prepared PS25-Lipo were sized by extrusion, followed by passing through a PD-10 column (Cytiva, Tokyo, Japan) to replace external ammonium sulfate with 20 mM *N*-(2-hydroxyethyl)piperazine-*N*′-2-ethanesulfonic acid (HEPES) (pH 8.0). The liposomes were enriched by ultracentrifugation (112500 × ***g***, 60 min, 4 °C), and resuspended with 20 mM HEPES (pH 8.0). The solution of DOX (Nacalai Tesque) was then mixed with the liposomes and incubated for 20 min at 37 °C. Calcium fusion of PS25-Lipo encapsulating DOX (PS-Lipo-DOX) and B16-sEVs was performed as described above, followed by ultracentrifugation to remove unencapsulated DOX. The amount of encapsulated DOX in PS-Lipo-DOX and CM-NP encapsulating DOX (CM-NP-DOX) was quantified by determining the absorbance ($\lambda = 484$ nm) following solubilizing the liposomes in 1% Triton-X100. Encapsulation efficiency of DOX was determined as the percentage of the amount of encapsulated DOX to that of the initially added DOX.

To evaluate DOX encapsulation efficiency into B16-sEVs by simple incubation, B16-sEVs (30 μg in 500 μL PBS) were mixed with 500 μL of 500 μM DOX solution dissolved in 20 mM HEPES (pH 8.0) and incubated for 90 min at 37 °C. The incubation ratio of B16-sEVs with DOX and incubation time were the same as the conditions for calcium fusion. After removing unencapsulated DOX by ultracentrifugation, encapsulation efficiency of DOX was determined as described above.

Cell Viability Assay B16F1 cells were seeded onto a 24-well plate (3×10^4 cells/well). After overnight incubation, DOX solution, PS-Lipo-DOX, or CM-NP-DOX was mixed with DMEM containing 10% FBS and added to the cells at final DOX concentrations of 0.3 and 3 μM. At 24 h after the sample addition, the cellular viability was assessed with a Cell Counting Kit-8 (Dojindo) in accordance with the manufacturer's instructions.

Statistical Analysis Statistical differences were analyzed by one-way ANOVA followed by the Tukey *post-hoc* test. Data are mean ± standard derivation (S.D.).

RESULTS AND DISCUSSION

We firstly prepared liposomes containing each ratio of PS (0, 10, 25, 50 mol% of total lipid) and investigated their membrane fusion with sEVs by the calcium fusion method. In our previous study, we found that the average particle number of B16-sEVs collected by the same procedure as the present study is $2.3 \pm 0.6 \times 10^9$ particles/μg (6.9×10^{10} particles/30 μg in 250 μL).[12] In this study, we also preliminarily evaluated the average particle number of 100 μM liposomes by using a nanoparticle multianalyzer (qNano; Meiwafosis Co., Ltd., Tokyo, Japan) and the average number was determined to be $2.7 \pm 1.7 \times 10^{11}$ particles/mL (6.8×10^{10} particles in 250 μL).

Table 1. Physicochemical Properties of the Liposomes, B16-sEVs, and CM-NP

Sample	Size (d. nm)	PDI	ζ-Potential (mV)
PS0-Lipo	136.4 ± 9.6	0.14 ± 0.06	−4.1 ± 1.3
PS10-Lipo	139.2 ± 15.2	0.15 ± 0.05	−12.8 ± 0.8
PS25-Lipo	122.4 ± 7.3	0.12 ± 0.02	−18.0 ± 1.4
PS50-Lipo	124.9 ± 8.7	0.15 ± 0.04	−21.8 ± 4.3
B16-sEVs	144.3 ± 26.1	0.30 ± 0.05	−23.7 ± 5.9
PS0-Lipo + B16-sEVs	531.1 ± 156.4	0.61 ± 0.19	−17.4 ± 2.9
PS10-Lipo + B16-sEVs	367.3 ± 22.9	0.68 ± 0.33	−20.3 ± 1.0
PS25-Lipo + B16-sEVs	379.6 ± 146.8	0.55 ± 0.09	−19.3 ± 3.9
PS50-Lipo + B16-sEVs	1387.1 ± 841.1	0.76 ± 0.18	−16.9 ± 3.1
PS-Lipo-DOX	164.9 ± 29.9	0.26 ± 0.07	−20.5 ± 4.1
CM-NP-DOX	334.2 ± 155.0	0.46 ± 0.04	−19.5 ± 1.9

Data represent mean ± S.D. ($n = 3$–4).

Based on these results, we incubated 250 μL (30 μg) of B16-sEVs and 250 μL of 100 μM liposomes for fusion to make the incubation ratio to be approximately 1 : 1. B16-sEVs was isolated by the ultracentrifugation method and used in this study. The particle size, PDI, and ζ-potential of each PS-Lipo and B16-sEVs are shown in Table 1. Membrane fusion efficiency of PS-Lipo labeled with NBD- and Rhodamine-DOPE and B16-sEVs was evaluated using FRET. As shown in Figs. 1A–D, NBD excitation at 460 nm induced Rhodamine emission around 590 nm in each PS-Lipo without fusion, indicating that both fluorophores are in close proximity and under the FRET condition in liposomal membranes before fusion. However, membrane fusion with B16-sEVs by the calcium fusion method, namely incubation with calcium ion and subsequent EDTA, largely decreased Rhodamine fluorescence in the groups using PS10-, PS25-, and PS50-Lipo (Figs. 1B–D). These results indicate that the distances between NBD and Rhodamine in the liposomal membranes increased due to membrane fusion-mediated lipid dilution, by which FRET efficiency decreased. The quantitative graph showed that the percentages of FRET fluorescence decrease after fusion was significantly larger in PS10-, PS25-, and PS50-Lipo groups than that of PS0-Lipo, and that was the highest in PS25-Lipo group (Fig. 1E). The increases in particle sizes of those nanoparticles also indicate an induction of membrane fusion by the calcium fusion (Table 1). A decrease in FRET fluorescence and an increase in particle size were also observed in the PS0-Lipo group, suggesting that a small amount of PS0-Lipo might also fuse together during the fusion between PS-presenting B16-sEVs. Although the detailed reason why PS50-Lipo + B16-sEVs showed higher ζ-potential than each nanoparticle is not clear, the particle size became quite large after calcium fusion possibly due to aggregation of the particles. Based on this result, it is speculated that calcium ions used for membrane fusion could not be completely chelated by EDTA from the aggregated particles and remained in the lipid membranes of PS50-Lipo and B16-sEVs, which might induce increase in ζ-potential of fused nanoparticles compared with PS50-Lipo and B16-sEVs. Considering the membrane fusion efficiency and particle size, we decided to use PS25-Lipo in the subsequent experiments, and the nanoparticles prepared by membrane fusion of PS25-Lipo and B16-sEVs were termed CM-NP. The data of particle size distribution of PS25-Lipo,

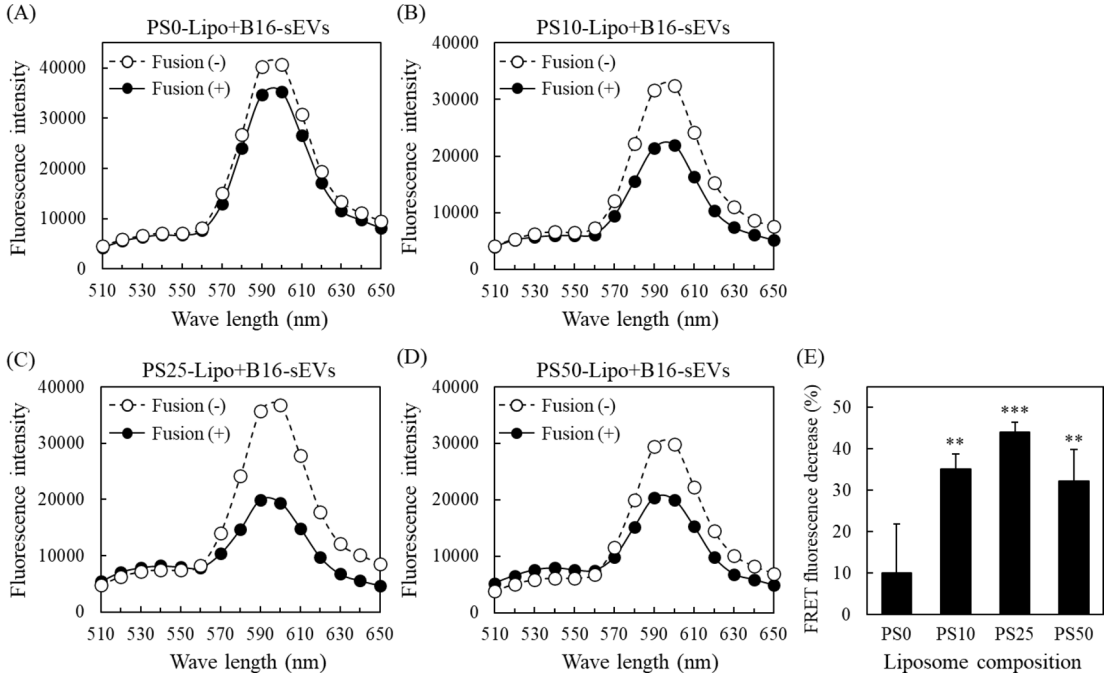

Fig. 1. Evaluation of Membrane Fusion of PS-Liposomes and B16-sEVs Using FRET

(A–D) Fluorescent spectra from 510 to 650 nm with excitation of NBD at 460 nm (A: PS0-Lipo + B16-sEVs, B: PS10-Lipo + B16-sEVs, C: PS25-Lipo + B16-sEVs, D: PS50-Lipo + B16-sEVs). The black (Fusion (+)) and dotted graphs (Fusion (−)) indicate the spectra of the samples subjected to calcium fusion or the same process without $CaCl_2$ and EDTA, respectively. The spectra are representative data from three independent experiments. (E) The decrease rate of the FRET fluorescence before/after membrane fusion are presented. Data are mean ± S.D. ($n = 3$). $^{**}p < 0.01$ and $^{***}p < 0.001$ *vs.* PS0.

B16-sEVs, and CM-NP were shown in Fig. 2. Although unfused PS25-Lipo and B16-sEVs showed relatively monodispersed particle distribution (Figs. 2A, B), the distribution became broad and polydisperse upon membrane fusion with PS25-Lipo and B16-sEVs *via* calcium fusion (Fig. 2C).

To more accurately confirm the formation of CM-NP, we next performed iodixanol density gradient ultracentrifugation fraction analysis. In this experiment, liposomes and B16-sEVs were labeled with Rhodamine-DOPE and PKH67, respectively, and the mixtures of each liposome and B16-sEVs were prepared with/without treatments for calcium fusion. In case of without fusion, the Rhodamine fluorescence derived from PS0- or PS25-Lipo was determined in fractions 1 and 2 (low-density fractions), and the PKH67 fluorescence from B16-sEVs was broadly detected from mostly fractions 4 to 10 (Fig. 3), as previously reported that sEVs possess a broad range of densities between 1.08–1.19 g/mL.[15] After fusion, the fraction of B16-sEVs was mainly determined in Fraction 8 (Fig. 3A) or 7–8 (Fig. 3B). Regarding the results of Fig. 3A (PS0-Lipo + B16-sEVs), we consider that each sEV containing PS fused with other sEVs, while PS0-Lipo not containing PS existed as liposomes without fusion with sEVs. Importantly, shift of the main liposomal fraction to the same fraction with B16-sEVs was observed when using PS25-Lipo (Fig. 3B), but not when using PS0-Lipo. These results indicate that lipid membranes of liposomes and sEVs coexisted in the same fractions in the state of CM-NP, although some population of sEVs might fuse with sEVs, not with PS25-Lipo. The membrane fusion efficiency was calculated by the percentage of Rhodamine fluorescence values in the liposome fractions coexisting with the sEVs fractions after fusion treatment to total Rhodamine fluorescence values observed in all fractions, and the efficiency was determined to be 66.7 ± 3.8% from the three independent results of this assay. These results further indicate that CM-NP was successfully prepared by calcium fusion of PS25-Lipo and B16-sEVs.

Next, cellular uptake of CM-NP into B16F1 cells, parental cells of B16-sEVs, was evaluated by fluorescence labeling of the samples with PKH67. The results of confocal microscopy showed that only a small amount of PKH67 fluorescence derived from PS25-Lipo was observed, while higher fluorescence was broadly observed in the group of B16-sEVs 24 h after the sample addition (Fig. 4A). Importantly, PKH67 fluorescence in B16F1 cells incubated with CM-NP was more intense than that of PS25-Lipo and comparable to the cells treated with B16-sEVs. By lysing the cells 6 or 24 h after sample addition, we also quantified PKH67 fluorescence in the cells and determined cellular uptake efficiency of each sample. Consistent with the results of confocal microscopy, the uptakes of B16-sEVs and CM-NP were significantly higher than that of PS25-Lipo at both 6 and 24 h, and similar uptake was observed between the groups of B16-sEVs and CM-NP (Fig. 4B). To investigate whether the proteins on B16-sEVs and CM-NP affected their cellular uptake into B16F1 cells, effect of Proteinase K treatment on the cellular uptake of B16-sEVs and CM-NP was evaluated, as reported previously.[16] The confocal images showed that treatment of B16-sEVs with Proteinase K significantly decreased their cellular uptake into B16-F1 cells (Supplementary Fig. 1(A)), suggesting that surface proteins on B16-sEVs could be responsible for uptake into B16-F1 cells. On the other hand, cellular uptake of CM-NP tended to decrease by Proteinase K treatment, but not significant (Supplementary Fig. 1(B)). These results suggest that the membrane proteins on B16-sEVs would be presented on the membrane surface of CM-NP after calcium fusion, and that the proteins might partly contribute to higher cellular uptake of CM-NP than PS25-Lipo, although detailed mechanisms are needed to be elucidated.

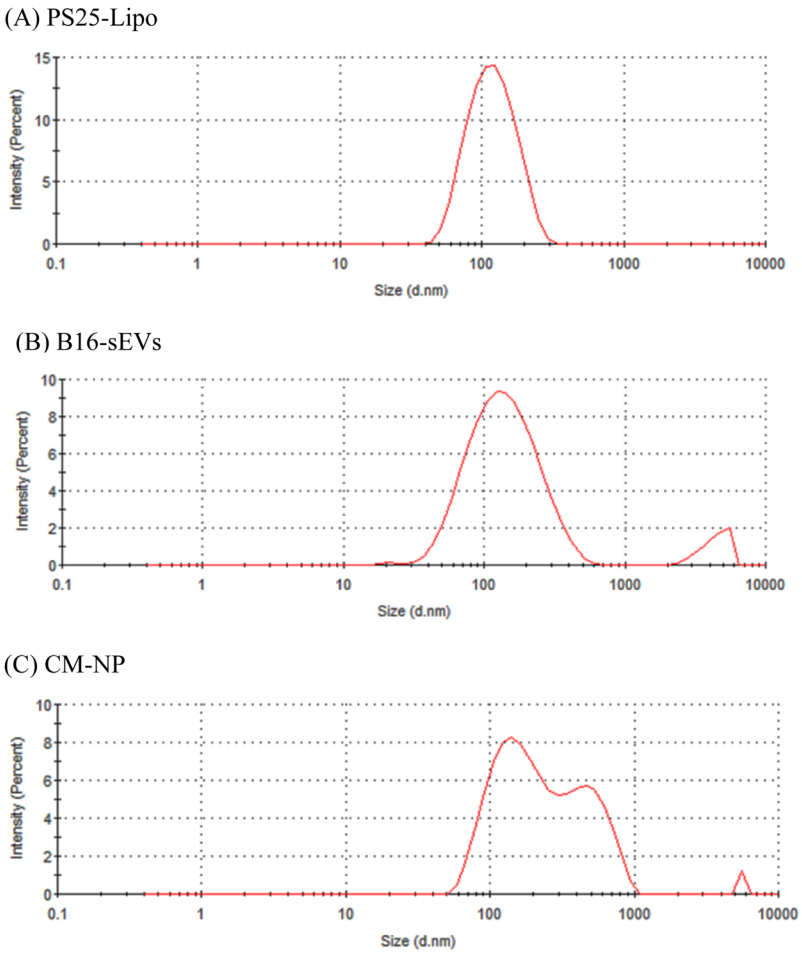

Fig. 2. Particle Size Distribution of PS25-Lipo, B16-sEVs, and CM-NP

The particle size distribution of PS25-Lipo (A), B16-sEVs (B), and CM-NP (C) were determined by using a Zetasizer Nano ZS.

Finally, CM-NP encapsulating an anticancer drug DOX (CM-NP-DOX) was prepared by membrane fusion of PS25-Lipo encapsulating DOX (PS-Lipo-DOX) and B16-sEVs, and we evaluated its growth inhibition effect on B16F1 cells. DOX encapsulation into PS25-Lipo was performed by the remote loading method using ammonium sulfate gradient, and membrane fusion with B16-sEVs was carried out after DOX encapsulation. The physicochemical properties of PS-Lipo-DOX and CM-NP-DOX are shown in Table 1. The DOX encapsulation efficiencies into PS25-Lipo and CM-NP were 71.3 ± 9.8 and $67.1 \pm 10.4\%$, respectively, and the efficiency was almost unchanged, regardless of the membrane fusion (Table 2). In the case of simple incubation of B16-sEVs and DOX solution, the DOX encapsulation efficiency was $5.2 \pm 0.6\%$ and the efficiency significantly increased by calcium fusion-mediated encapsulation method (Table 2), indicating that calcium fusion-mediated DOX encapsulation into sEVs should be a superior approach compared with the conventional simple incubation method. Treatment with CM-NP-DOX exhibited the highest anti-proliferative effect among the groups, and significantly decreased cell viability compared with DOX solution at $0.3\,\mu$M and PS-Lipo-DOX at $3\,\mu$M (Fig. 5). Based on the results of Figs. 3 and 4, it was suggested that higher uptake of CM-NP into B16F1 cells brought about greater anti-proliferative effect than PS25-Lipo. Although CM-NP-DOX exhibited higher anti-proliferative effect than PS-Lipo-DOX, the difference was not so different compared to the differences in cellular uptake. Lipid composition of liposomes is considered to be one of the reasons. In this study, we prepared DOX-encapsulated liposomes composed of two unsaturated phospholipids, namely EPC and DOPS, without using cholesterol which contributes to liposomal membrane stabilization. It was previously reported that DOX-encapsulated liposomes composed of EPC/cholesterol (2/1 M ratio) released only 14% of encapsulated DOX after 24 h incubation in HEPES-buffered saline, whereas the liposomes composed only EPC released 47% of encapsulated DOX, indicating that drug release from liposomes composed of only unsaturated phospholipids is quite rapid.[17] Based on this finding, we consider that DOX release from PS25-Lipo and CM-NP was fast, which made it difficult to see drastic differences between groups, although cellular uptake was more than two times higher than that of PS25-Lipo. Another possibility is that the average particle size of CM-NP-DOX (334.2 ± 155.0 nm) was higher than that of PS-Lipo-DOX (164.9 ± 29.9 nm) and the higher particle size might affect intracellular distribution of nanoparticles and encapsulated DOX upon cellular uptake. In this study, we focused on membrane fusion of PS-Lipo and sEVs by calcium fusion method and its application for drug encapsulation; however, since optimization of lipid composition of PS-Lipo is essential for *in vivo* application of CM-NP, we would definitely try in future study to demonstrate further usefulness of CM-NP. Until now, a few methods, such as repeated freeze-thawing and the use of polyethylene glycol as a cellular fusion

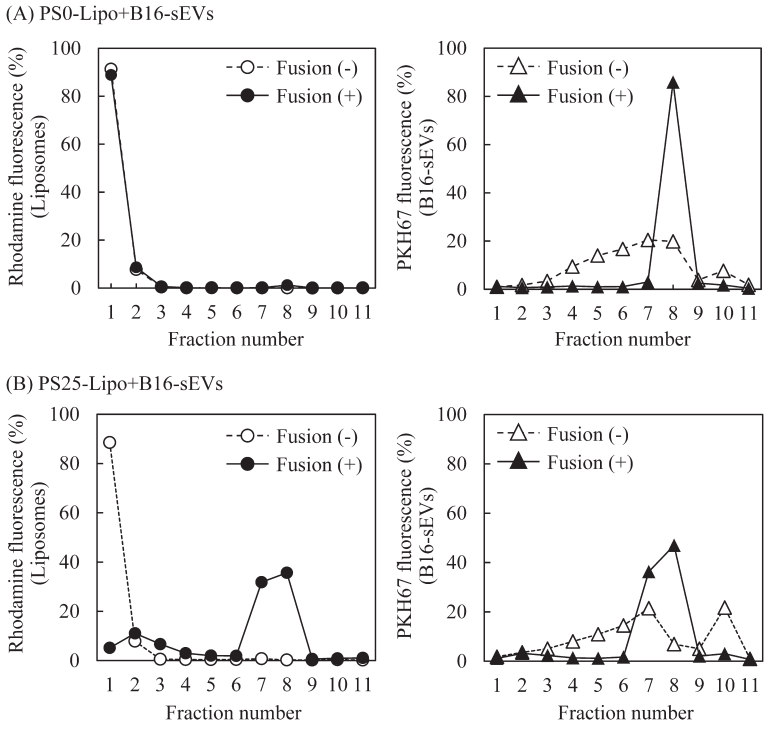

Fraction number	1	2	3	4	5	6	7	8	9	10	11
Density (g/mL)	1.02	1.05	1.08	1.10	1.12	1.13	1.14	1.15	1.17	1.20	1.26

Fig. 3. Confirmation of Membrane Fusion of PS25-Lipo and B16-sEVs by a Density Gradient Ultracentrifugation Analysis

(A, B) Each liposome and B16-sEVs were labeled with Rhodamine-DOPE and PKH67, respectively. The Rhodamine-labeled PS0-Lipo or PS25-Lipo were mixed with PKH67-labeled B16-sEVs and those mixtures were subjected to a density gradient ultracentrifugation after calcium fusion. Fluorescence intensities of Rhodamine-labeled liposomes (open circle plus dotted line: without fusion, closed circle plus black line: with fusion) and PKH67-labeled B16-sEVs (open triangle plus dotted line: without fusion, closed triangle plus black line: with fusion) in each fraction were measured. The table below the graphs represents the density of each fraction determined as previously reported.[20]

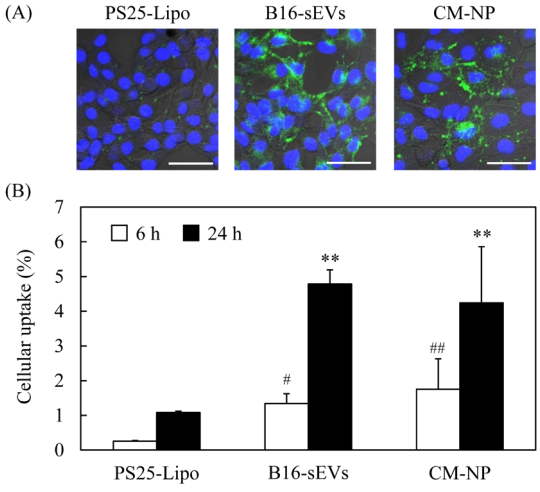

Fig. 4. Cellular Uptake of PS25-Lipo, B16-sEVs, and CM-NP into B16F1 Melanoma Cells

(A) B16F1 cells were incubated with PKH67-labeled PS25-Lipo, B16-sEVs, or CM-NP (Final conc.: 10 μg/mL as B16-sEVs and 8.3 μM as PS25-Lipo in DMEM supplemented with 10% FBS). After incubation for 24 h, uptake of each sample was determined with a confocal laser scanning microscope following nuclear staining with DAPI solution. Blue and green colors present fluorescence of DAPI (nuclei) and PKH67 (samples), respectively. Scale bars = 50 μm. (B) For quantification of the uptake efficiency of the samples, the PKH67 fluorescence intensity was determined by lysing the treated cells 6 and 24 h after sample addition. Data are mean ± S.D. ($n = 4$). Significant differences: $^{\#}p < 0.05$ $^{\#\#}p < 0.01$ *vs.* PS25-Lipo (6 h) and $^{**}p < 0.01$ *vs.* PS25-Lipo (24 h).

Table 2. DOX Encapsulation Efficiency into PS25-Lipo, CM-NP, and B16-sEVs by the Indicated Encapsulation Methods

Sample	DOX encapsulation ratio (%)
PS25-Lipo (Remote loading)	71.3 ± 9.8***
CM-NP (Calcium fusion)	67.1 ± 10.4***
B16-sEVs (Simple incubation)	5.2 ± 0.6

DOX encapsulation into PS25-Lipo, CM-NP, and B16-sEVs was performed by remote loading, calcium fusion, and simple incubation method, respectively, as mentioned in Material and Methods (Preparation of CM-NP encapsulating doxorubicin). Data represent mean ± S.D. ($n = 3$–5). Significant differences: $^{***}p < 0.001$ *vs.* B16-sEVs (Simple incubation).

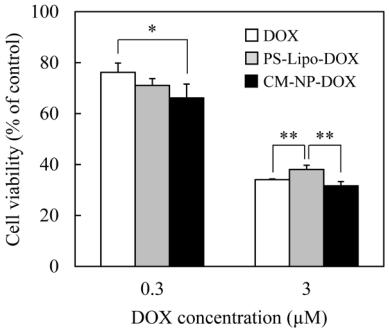

Fig. 5. Anticancer Effect of CM-NP-DOX against B16F1 Cells

B16F1 cells were treated with DOX solution, PS-Lipo-DOX, or CM-NP-DOX (Final DOX conc.: 0.3 and 3 μM in DMEM supplemented with 10% FBS). Cell viability was assessed after 24 h incubation using the WST-8 assay. Data are the mean ± S.D. ($n = 4$). Significant differences: $^{*}p < 0.05$, $^{**}p < 0.01$.

reagent, have been reported for fusion of sEVs and liposomes to prepare functional nanoparticles.[18] The present findings may offer a new approach to prepare sEV-based nanoparticles by PS-mediated calcium fusion method.

To demonstrate further usefulness of the CM-NP prepared by the calcium fusion method, therapeutic application *in vivo* is necessary, while particle size regulation is an issue to be solved for systemic administration. We recently reported that high-pressure homogenization with a microfluidizer decreases the particle size of sEVs without influence on their morphology and apparent function, and enables simultaneous loading of small molecular anticancer drugs and functional lipid into sEVs, which allows for effective cancer therapy by systemic injection of the prepared sEVs.[19] Combination of the calcium fusion and the microfluidizer may be a promising approach for particle size regulation of CM-NP and increase in their functionalities. Additionally, to further demonstrate the advantage of the calcium method, encapsulation of macromolecular drugs, such as small interfering RNA (siRNA) and protein drugs, should be the next step since encapsulation of those drugs into sEVs has required to be improved due to some issues such as low encapsulation efficiency and poor reproducibility.[5] In this study, we focused on demonstrating whether liposomes composed of PS can be fused with sEVs by calcium fusion and whether the calcium fusion can be applied to drug encapsulation by using DOX as a model low-molecular drug because DOX is easily encapsulated into liposomes. Consequentially, we could successfully suggest the usefulness of calcium fusion as an approach to the encapsulation of therapeutic drugs into sEVs *via* membrane fusion with liposomes composed of PS. In future study, we would definitely like to try the encapsulation of macromolecular drugs into sEVs *via* calcium fusion while regulating the particle size of the resultant CM-NP.

In conclusion, we have demonstrated that the calcium fusion method can be applied for membrane fusion of PS-liposomes and sEVs which contain PS in their lipid membranes. This approach could be useful for efficient drug encapsulation into sEVs and increase in the functionalities of liposomes.

Acknowledgments The present research was funded by JSPS KAKENHI (21K18065) and the Asahi Glass Foundation. This research was also supported by the Research Program for the Development of Intelligent Tokushima Artificial Exosome (iTEX) from Tokushima University. We acknowledge proofreading and editing of a draft of this manuscript by Benjamin Phillis at Wakayama Medical University.

Conflict of Interest The authors declare no conflict of interest.

Supplementary Materials This article contains supplementary materials.

REFERENCES

1) Colombo M, Raposo G, Thery C. Biogenesis, secretion, and intercellular interactions of exosomes and other extracellular vesicles. *Annu. Rev. Cell Dev. Biol.*, **30**, 255–289 (2014).
2) Rezaie J, Feghhi M, Etemadi T. A review on exosomes application in clinical trials: perspective, questions, and challenges. *Cell Commun. Signal.*, **20**, 145 (2022).
3) Hoshino A, Costa-Silva B, Shen T-L, *et al.* Tumour exosome integrins determine organotropic metastasis. *Nature*, **527**, 329–335 (2015).
4) Li C, Qin S, Wen Y, Zhao W, Huang Y, Liu J. Overcoming the blood-brain barrier: exosomes as theranostic nanocarriers for precision neuroimaging. *J. Control. Release*, **349**, 902–916 (2022).
5) Rankin-Turner S, Vader P, O'Driscoll L, Giebel B, Heaney LM, Davies OG. A call for the standardised reporting of factors affecting the exogenous loading of extracellular vesicles with therapeutic cargos. *Adv. Drug Deliv. Rev.*, **173**, 479–491 (2021).
6) Chen H, Wang L, Zeng X, Schwarz H, Nanda HS, Peng X, Zhou Y. Exosomes, a new star for targeted delivery. *Front. Cell Dev. Biol.*, **9**, 751079 (2021).
7) Fukuta T, Oku N, Kogure K. Application and utility of liposomal neuroprotective agents and biomimetic nanoparticles for the treatment of ischemic stroke. *Pharmaceutics*, **14**, 361 (2022).
8) Itani T, Ariga H, Yamaguchi N, Tadakuma T, Yasuda T. A simple and efficient liposome method for transfection of DNA into mammalian cells grown in suspension. *Gene*, **56**, 267–276 (1987).
9) Papahadjopoulos D, Nir S, Düzgünes N. Molecular mechanisms of calcium-induced membrane fusion. *J. Bioenerg. Biomembr.*, **22**, 157–179 (1990).
10) Skotland T, Hessvik NP, Sandvig K, Llorente A. Exosomal lipid composition and the role of ether lipids and phosphoinositides in exosome biology. *J. Lipid Res.*, **60**, 9–18 (2019).
11) Nakai W, Yoshida T, Diez D, Miyatake Y, Nishibu T, Imawaka N, Naruse K, Sadamura Y, Hanayama R. A novel affinity-based method for the isolation of highly purified extracellular vesicles. *Sci. Rep.*, **6**, 33935 (2016).
12) Fukuta T, Nishikawa A, Kogure K. Low level electricity increases the secretion of extracellular vesicles from cultured cells. *Biochem. Biophys. Rep.*, **21**, 100713 (2020).
13) Scott BL, Van Komen JS, Liu S, Weber T, Melia TJ, McNew JA. Liposome fusion assay to monitor intracellular membrane fusion machines. *Methods Enzymol.*, **372**, 274–300 (2003).
14) Fukuta T, Yoshimi S, Kogure K. Leukocyte-Mimetic Liposomes Penetrate Into Tumor Spheroids and Suppress Spheroid Growth by Encapsulated Doxorubicin. *J. Pharm. Sci.*, **110**, 1701–1709 (2021).
15) Brennan K, Martin K, FitzGerald SP, O'Sullivan J, Wu Y, Blanco A, Richardson C, Mc Gee MM. A comparison of methods for the isolation and separation of extracellular vesicles from protein and lipid particles in human serum. *Sci. Rep.*, **10**, 1039 (2020).
16) Charoenviriyakul C, Takahashi Y, Morishita M, Nishikawa M, Takakura Y. Role of extracellular vesicle surface proteins in the pharmacokinetics of extracellular vesicles. *Mol. Pharm.*, **15**, 1073–1080 (2018).
17) Mayer LD, Tai LC, Ko DS, Masin D, Ginsberg RS, Cullis PR, Bally MB. Influence of vesicle size, lipid composition, and drug-to-lipid ratio on the biological activity of liposomal doxorubicin in mice. *Cancer Res.*, **49**, 5922–5930 (1989).
18) Mondal J, Pillarisetti S, Junnuthula V, Saha M, Hwang SR, Park IK, Lee YK. Hybrid exosomes, exosome-like nanovesicles and engineered exosomes for therapeutic applications. *J. Control. Release*, **353**, 1127–1149 (2023).
19) Fukuta T, Ikeda-Imafuku M, Kodama S, Kuse J, Matsui K, Iwao Y. One-step pharmaceutical preparation of PEG-modified exosomes encapsulating anti-cancer drugs by a high-pressure homogenization technique. *Pharmaceuticals*, **16**, 108 (2023).
20) Ji H, Greening DW, Barnes TW, Lim JW, Tauro BJ, Rai A, Xu R, Adda C, Mathivanan S, Zhao W, Xue Y, Xu T, Zhu HJ, Simpson RJ. Proteome profiling of exosomes derived from human primary and metastatic colorectal cancer cells reveal differential expression of key metastatic factors and signal transduction components. *Proteomics*, **13**, 1672–1686 (2013).